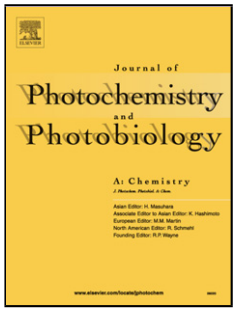

Title: Photocatalytic ozonation of monuron over suspended and immobilized TiO_2–study of transformation, mineralization and economic feasibility

Authors: Gergő Simon, Tamás Gyulavári, Klára Hernadi, Milán Molnár, Zsolt Pap, Gábor Veréb, Krisztina Schrantz, Máté Náfrádi, Tünde Alapi

PII: S1010-6030(17)31769-0
DOI: https://doi.org/10.1016/j.jphotochem.2018.01.025
Reference: JPC 11113

To appear in: *Journal of Photochemistry and Photobiology A: Chemistry*

Received date: 10-12-2017
Revised date: 11-1-2018
Accepted date: 16-1-2018

Please cite this article as: Gergő Simon, Tamás Gyulavári, Klára Hernadi, Milán Molnár, Zsolt Pap, Gábor Veréb, Krisztina Schrantz, Máté Náfrádi, Tünde Alapi, Photocatalytic ozonation of monuron over suspended and immobilized TiO2–study of transformation, mineralization and economic feasibility, Journal of Photochemistry and Photobiology A: Chemistry https://doi.org/10.1016/j.jphotochem.2018.01.025

Photocatalytic ozonation of monuron over suspended and immobilized TiO_2 – study of transformation, mineralization and economic feasibility

Gergő Simon[a,b,c], Tamás Gyulavári[b,d], Klára Hernadi[b,d], Milán Molnár[a,c], Zsolt Pap[b,e,f,g], Gábor Veréb[b,h], Krisztina Schrantz[a,c], Máté Náfrádi[a,c], Tünde Alapi[a,c]*

[a]*Research Group of Environmental Analytical Chemistry, Institute of Chemistry, University of Szeged, H-6720, Dóm tér 7, Szeged, Hungary*

[b]*Research Group of Environmental Chemistry, Institute of Chemistry, University of Szeged; H-6720, Tisza Lajos krt. 103., Szeged, Hungary*

[c]*Department of Inorganic and Analytical Chemistry, Institute of Chemistry, University of Szeged, Dóm tér 7, H-6720 Szeged, Hungary*

[d]*Department of Applied and Environmental Chemistry, Institute of Chemistry, University of Szeged, Rerrich Béla tér 1, H-6720 Szeged, Hungary*

[e]*Faculty of Physics, Babeş–Bolyai UniversityM. Kogălniceanu 1, RO–400084 Cluj–Napoca, Romania*

[f]*Institute for Interdisciplinary Research on Bio-Nano-Sciences, Treboniu Laurian 42, RO–400271 Cluj-Napoca, Romania*

[g]*Institute of Environmental Science and Technology, University of Szeged, Tisza Lajos krt. 103, Szeged HU-6720, Hungary*

[h]*Department of Process Engineering, Faculty of Engineering, University of Szeged Moszkvai krt. 9., H-6725 Szeged, Hungary*

*Corresponding author: tel.: +36-62-54-4719, e-mail: *alapi@chem.u-szeged.hu*
Address: H-6720 Szeged, Dóm tér 7, Hungary

Graphical abstract

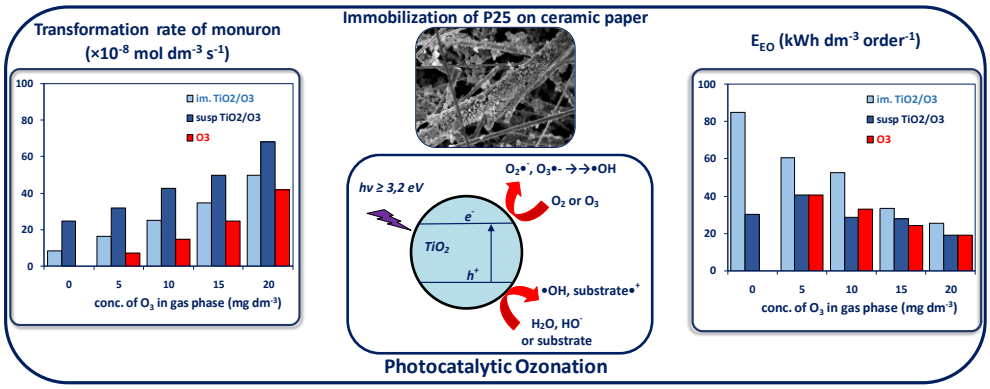

Highlights

- addition of O_3 increased the transformation and mineralization rate of monuron
- TiO_2 decreased the concentration of dissolved O_3
- synergism was not observed in the transformation or mineralization rate of monuron
- synergism manifested in the energy requirement of mineralization using susp-TiO_2/O_3

Abstract

The transformation and mineralization of monuron herbicide were investigated by heterogeneous photocatalysis, ozonation, and their combination (photocatalytic ozonation) at various ozone (O_3) concentrations (0–20 mg·dm^{-3} in gas phase), using TiO_2 in suspensions and in immobilized form.

The applied AOPs were characterized by the transformation and mineralization rate of monuron, the concentration of dissolved O_3, and the economic feasibility based on the values of Electrical Energy per Order related to the rate of decrease of monuron concentration and of the total organic carbon content. In the case of photocatalytic ozonation, the transformation and mineralization rate of monuron increased with the increase of O_3 concentration. However, there was no significant synergistic effect. Electrical Energy per Order decreased with the increase of O_3 concentration, and economical efficiency of the photocatalytic ozonation using TiO_2 in suspensions highly exceed that of both ozonation and heterogeneous photocatalysis regarding the value determined for the decrease of total organic carbon content.

Keywords: TiO_2 immobilization, monuron, photocatalysis, photocatalytic ozonation, ozone, Electric Energy per Order

1. Introduction

Although necessary, the application of pesticides can have severe negative effects for environmental systems, resulting in their accumulation in soil and appearance in waters, including drinking waters. Moreover, a number of these compounds are supposed or proven carcinogens, mutagens or endocrine disruptors (Bonnemoy et al., 2004; Benitez et al., 2009; Mestankova et al., 2011; Kottuparambil et al., 2013). Their removal from waters therefore is an important task, which can be achieved through the application of advanced oxidation processes (AOPs). The degradation of monuron (*3*-(*p*-chlorophenyl)-*1,1*-dimethylurea) and phenylurea pesticides in general has been studied using several methods, such as photolysis (Kovács et al., 2016a), gamma-radiolysis (Kovács et al., 2014b; Kovács et al., 2016b). electro– and photo–Fenton processes (Bobu et al., 2006; Oturan et al., 2010), ozonation (Tahmasseb et al., 2002; Kovács et al., 2016a), heterogeneous photocatalysis (Rao et al., 2010; Chu et al., 2012; Solís et al., 2016) or their combinations including photocatalytic ozonation (Bobu et al., 2006; Oturan et al., 2010)

Titanium dioxide (TiO_2) is generally considered the most adequate photocatalyst, as it is cheap, inert, and it has prominent photocatalytic activity. After the treatment, it is necessary to separate the TiO_2 particles, increasing the operation-cost of heterogeneous photocatalysis as water treatment method. Therefore, numerous attempts have been made to immobilize photocatalysts on various support materials (Krýsa et al., 2006; Behnajady et al., 2008; Tryba, 2008; Zhang et al., 2015). Moreover, immobilization of photocatalyst opens the possibility of heterogeneous photocatalysis application in continuous flow system. The photocatalyst particles can be immobilized onto the surface via several techniques, like dip-coating (Giornelli et al., 2007; Hosseini et al., 2007; Behnajady et al., 2008; Khataee et al., 2013), embedding the photocatalyst particles into polymers (Naskar et al., 1998; Fabiyi et al., 2000; Baudys et al., 2017), and also by electrophoretic deposition (Dunlop et al., 2008). While these methods use pre-made photocatalysts, there are processes, such as the sol-gel process (Balasubramanian et al., 2004; Gelover et al., 2004), or the chemical vapor deposition (Karches et al., 2002; Puma et al., 2008; Zhang et al., 2008), where the catalyst particles are formed *in situ*, thus their properties are more difficult to control.

While ozonation and heterogeneous photocatalysis are effective processes separately, their combination – photocatalytic ozonation – can have a synergistic effect both in oxidation and mineralization efficiency (Ilisz et al., 2004; Beltrán et al., 2005; Farré et al., 2005). Despite of the additional electrical energy for ozone generation, several publications proved that heterogeneous photocatalytic ozonation may be a cost-effective alternative for wastewater

treatment primarily because of the shortened treatment time. (Kopf et al., 2000; Mehrjouei et al., 2014b). Synergistic effect was reported in the transformation and mineralization rate of various target substances (Jing et al., 2011; Aguinaco et al., 2012; Xiao et al., 2015; Fathinia et al., 2016) in aqueous solutions. The pH depending synergistic effect was demonstrated in the case of neonicotinoid insecticides (Černigoj et al., 2007). However Farré et al. (2005) reported that, there is no enhanced efficiency in the case of diuron and clofenvinphos, and only the mineralization was enhanced for nitrogen containing compounds (Klare et al., 1999). No enhanced efficiency was observed neither for transformation nor for the degradation rate of dichlorophenol (Melián et al., 2013) and Triton X-100 non-ionic surfactant (Hegedűs et al., 2015) using the combination of ozonation and heterogeneous photocatalysis.

Using UV irradiated TiO_2 the transformation of organic substances can occur via direct charge transfer or via $^{\bullet}OH$ based reaction. The enhanced efficiency of photocatalytic ozonation can be explained by the considerably higher electron affinity of ozone (O_3) compared to oxygen (O_2) (Pichat et al., 2000; Mehrjouei et al., 2015). Thus, the role of O_3 as a more effective electron trap, must be considered. O_3 adsorbs onto the surface of TiO_2 via Lewis acid sites (dissociative adsorption) or by weak hydrogen bonds, resulting in active oxygen radicals ($O^{\bullet}$), which produce $^{\bullet}OH$ by reacting with water molecules (Mehrjouei et al., 2015). The generation of one $^{\bullet}OH$ consumes only one electron due to the transformation of O_3 on the surface of TiO_2, while using O_2 three electrons are needed (Sánchez et al., 1998; Klare et al., 1999). Consequently, the positive effect of O_3 can originated in two reasons: the enhanced separation and lifetime of photogenerated charges and higher formation rate of $^{\bullet}OH$.

The goal of this study is to investigate the degradation and mineralization of the phenylurea herbicide monuron (*3*-(*p*-chlorophenyl)-*1,1*-dimethylurea) by ozonation, heterogeneous photocatalysis – in TiO_2 suspensions and using self-made immobilized TiO_2 sheets – and their combination (photocatalytic ozonation) at various O_3 concentrations. The possibility of the synergistic effect was investigated through the transformation and mineralization rate of monuron. The quality and quantity of byproducts was also investigated. The economic feasibility of treatments was compared based on the obtained values of Electrical Energy per Order (E_{EO}) determined for the decrease of monuron concentration and total organic carbon content.

2. Materials and methods

2.1. Materials

Aeroxide P25® (73-85 % anatase and 14-17 % rutile (Ohtani et al., 2010), S_{BET} = 35–65 $m^2 \cdot g^{-1}$, $d_{anatase}$~25 nm, d_{rutile}~40 nm, Evonik Industries) was used either in suspension or immobilized onto a high-purity alumina based ceramic paper (1.6 mm thickness, cat. no.: 300-040-1, COTRONICS Co.). The immobilization process involved titanium ethoxide ($Ti(OEt)_4$, technical grade, Sigma-Aldrich) as fixing agent, and isopropyl alcohol (laboratory grade, VWR). High purity nitrogen gas (99.995 %, Messer) was used to spray the TiO_2 suspensions onto the surface.

The model compound was monuron (Fig. 1) (> 99 %, Sigma-Aldrich), the initial concentration was 0.5 $mmol \cdot dm^{-3}$ in all experiments. The initial concentration of MeOH (HPLC pure, VWR) – used as hydroxyl radical scavenger – was 50 times higher, 250 $mmol \cdot dm^{-3}$.

Oxygen (99.5 %, Messer) was used to saturate the aqueous solutions and to produce O_3. Indigo carmine dye (high purity, Janssen Chimica), $NaH_2PO_4 \cdot 2H_2O$ (99.0 %, Sigma-Aldrich) and $Na_2HPO_4 \cdot 2H_2O$ (99.0 %, Sigma-Aldrich) were used for the dissolved O_3 determination. For the total organic carbon (TOC) determination ortophosphoric acid (analytical grade, 85 wt. %, VWR) and high purity oxygen (99.9995 %, Messer) were used. Solutions were prepared in ultrapure Milli-Q water.

2.2. Preparation of the immobilized catalysts

The immobilization of TiO_2 was carried out following the method described by Veréb et al. (2014). The ceramic paper sheets (34.0×14.0 cm; 476.0 cm^2) were immersed in isopropyl alcohol, coated with $Ti(OEt)_4$ and evenly sprayed with isopropanol based TiO_2 suspension (c_{P25} = 76.9 $g \cdot dm^{-3}$). Three ceramic papers – named P25-1, P25-2 and P25-3 – were made, having 0.777; 1.555 and 2.332 mg cm^{-2} immobilized Aeroxide P25® on the surface by spraying various volumes (4.8, 9.6 and 14.4 cm^3, respectively) of the TiO_2 suspension. The prepared sheets were dried for 24 h at room temperature. The amorphous titanium oxide hydroxide formed partly covers and strongly fixes the Aeroxide P25® particles to the surface of the ceramic paper. The prepared sheets were illuminated with 365 nm light for 24 h to evaporate the residual volatile compounds (mainly alcohols) and elimination of organic matter adsorbed on the surface via heterogeneous photocatalysis.

The transformation of monuron was investigated using photocatalyst in suspensions and in immobilized form in the reactor presented in section 2.4. Using 500 cm^3 (total volume of the reactor) suspension having 1.0, 2.0 and 3.0 $g \cdot dm^{-3}$ TiO_2 concentrations, the amount of TiO_2 in

the irradiated volume (370 cm^3) were the same than the amount of TiO_2 fixed on the ceramic papers named P25-1, P25-2 and P25-3.

2.3. Analytical methods

Scanning Electron Microscopy (SEM) measurements were made using a Hitachi S-4700 Type II FE-SEM instrument, which operates using a cold field emission gun (5-15 kV).

The X-ray diffractograms (XRD) were taken by a Rigaku Miniflex II diffractometer using Cu-Kα radiation (λ = 1.5406 Å), equipped with a graphite monochromator. Data points were taken in the 2θ = 20–40 ° range at a scan speed of $1 \cdot min^{-1}$. A series of calibration samples were prepared from ceramic sheets milled and mixed with calculated amounts of Aeroxide® P25. From the XRD patterns, the anatase diffraction peak at 25.6 ° was integrated, and calibration was based on the peak area. Ceramic sheets containing the immobilized P25 were treated similarly to the calibration samples.

A JASCO-V650 spectrophotometer with an integration sphere (ILV-724) was used for measuring the diffuse reflectance spectra (DRS) of the samples (λ = 300–800 nm). The possible electron transitions were evaluated by plotting the dR/dλ vs. λ, where R is the reflectance and λ is the wavelength (Pap et al., 2014).

Agilent 8435 UV-Vis spectrophotometer was used to measure the concentration of gaseous O_3 at 254 nm wavelength ($\varepsilon_{254\ nm} = 2950\ mol^{-1} \cdot dm^3 \cdot cm^{-1}$ (Hart et al., 1983)), using a 1.0 cm quartz flow-through cell at 500 $cm^3 \cdot min^{-1}$ gas flow.

The concentration of monuron was determined by high performance liquid chromatography (HPLC), using an Agilent 1100 modular HPLC system with a LiChroCART® C-18 column (250×4 mm, 5 µm particle size) equipped with a diode array detector (DAD) detector. The measurements were made at 25 °C using a mixture of methanol and water mixture (60:40 V/V %) as eluent at 1.0 $cm^3 \cdot min^{-1}$ flow rate. The quantification wavelength was 244 nm. The intermediates were separated and detected by the same HPLC system equipped with Agilent G1956A quadrupole mass spectrometric (MS) detector. The MS analysis was carried out in positive and negative ion modes, with an electrospray ionization source (ESI) using 70 and 90 V fragmentor voltages.

The TOC analyses were carried out using an Analytik Jena multi N/C® 3100 apparatus equipped with NDIR detector. The furnace temperature was 800 °C and 1.0 cm^3 samples were injected. Three parallel measurements were made in each case.

The concentration of dissolved O_3 was determined spectrophotometrically by the indigo carmine method (Bader et al., 1981; Chiou et al., 1995).

2.4. Photoreactor

All experiments were performed in the same photoreactor (SUP1). The light source was a fluorescent UV lamp (15 W, GCL303T5/365 nm, LightTech), which emits photons with wavelengths of 300-400 nm with a radiation maximum at 365 nm (SUP2). The photon flux ($1.20(\pm0.06)\cdot10^{-5}$ $mol_{photon}\cdot s^{-1}$) was determined by potassium ferrioxalate actinometry (Hatchard et al., 1956). UV lamp with the perforated glass envelope (length 320 mm and internal diameter 28 mm) was centred in the water-cooled, tubular glass reactor (length 340 mm, internal diameter 46 mm, volume 370 cm^3). The reactor was closed with a screw-off Teflon top fixed to the light source and its envelope. In case of heterogeneous photocatalysis (using suspended TiO_2 (susp-TiO_2) or immobilized TiO_2 containing ceramic sheet (34.0×14.0 cm) fitted to the inside wall of the reactor (imm-TiO_2)) oxygen (O_2), while in the case of ozonation and the combined methods (susp-TiO_2/O_3 and imm-TiO_2/O_3) O_3 containing O_2 gas was lead into the reactor through the Teflon packing ring. An ozonizer (Ozomatic Modular 4HC, max. 95 W) was used to produce O_3. Thus, O_2 or O_3 was lead between the wall of the fluorescent lamp and the perforated glass envelope, and bubbled through the irradiated volume of solution/suspension. The solutions were saturated with O_2 for 10 minutes before the kinetic measurements, which were started by switching on the light source and ozonizer. The thermostated (25±0.5 °C) monuron solution (500 cm^3, $5.0\cdot10^{-4}$ $mol\cdot dm^{-3}$) was circulated (375 $cm^3\cdot min^{-1}$) continuously and stirred in the reservoir. The formal initial transformation rates of monuron were obtained by linear regression fitting to the initial, linear segment of the kinetic curves. Kinetic measurements (heterogeneous photocatalysis (using TiO_2 in both suspended and immobilized form), ozonation and combination of methods were repeated three times, to check their reproducibility.

2.5. Electrical Energy per Order

When choosing the best method for wastewater treatment, some significant factors should be taken under consideration. The economic factor is often seen as the most relevant as AOPs are electric-energy-intensive methods (Bolton et al., 2001). To compare the economic efficiency of the applied AOPs the values of Electrical Energy per Order **(**E_{EO}) were calculated for both monuron transformation **(**E_{EO}^{c}) and mineralization **(**E_{EO}^{TOC}). Calculation is based on the standard figures of-merit for the comparison of energy established regardless of the nature of the system, developed by Bolton et al. (2001). The amount of electric energy is required to decrease the concentration of pollutant by one order of magnitude. The effectiveness of each

process was evaluated based on these E_{EO} values reflecting the electric energy in kilowatt hours [kWh] required to treat 1 m^3 of contaminated water (Bolton et al., 2001). E_{EO} values [$kWh \cdot m^{-3} \cdot order^{-1}$] are calculated using the following formula in a batch system:

$$E_{EO}{}^{c} = \frac{P \times t \times 1000}{V \times \lg(c_i/c_f)} \quad (1)$$

$$E_{EO}{}^{TOC} = \frac{P \times t \times 1000}{V \times \lg(TOC_i/TOC_f)} \quad (2)$$

where P is the rated power [kW] of the AOT the system, V is the volume [dm^3] of water treated, t [h] is the time required to decrease the concentration of pollutant (c_i and c_f are the initial and final concentrations of monuron [$mol \cdot dm^{-3}$], while TOC_i and TOC_f are the initial and final TOC content [$mol \cdot dm^{-3}$]) by one order of magnitude, and *lg* is the symbol for the decadic logarithm. The determination of t necessary for the monuron concentration or TOC decrease from c_i to c_f and TOC_i to TOC_f, when necessary, was based on extrapolation of the measured data.

In the present work the power (P) was calculated by the sum of the electric power required for the UV lamp (15 W) and the power needed for ozonizer to generate required O_3 concentrations (9.3, 13.8, 18.3, 22.8 W to generate 5.0, 10.0, 15.0, 20.0 $mg \cdot dm^{-3}$ O_3 in gas phase, respectively). Similar calculation was presented by Mehrjouei et al. (2014a, b) and Cardoso et al. (2016).

3. Results and discussion

3.1. Characterization of the immobilized TiO_2 containing ceramic sheets

The structural and optical analyses were made to verify the success of the immobilization, to determine the possible changes in optical properties and the exact amount of immobilized TiO_2 on the ceramic sheets. SEM micrographs provided direct evidence of the successful immobilization of TiO_2 nanoparticles on the surface of the ceramic paper. Increasing the amount of the immobilized photocatalyst, larger aggregates of nanoparticles were detected (Fig. 2).

XRD measurements were performed in order to determine the amount of P25 fixed on the ceramic sheets (Table 1. and SUP3.). The amount of TiO_2 immobilized was calculated from the volume and concentration of TiO_2 suspension sprayed during the process of immobilization (calculated amount). The determination of the immobilized TiO_2 amount was

based on XRD data (measured amount) and verified that, the amount of immobilized TiO_2 correspond well to the calculated values (Table 1).

To verify the optical properties of the ceramic papers, DRS spectra were recorded (Fig. 3). In case of the $Ti(OEt)_4$ impregnated sheet the band-gap value calculated according to (Flak et al., 2013; Baia et al., 2014; Kovács et al., 2014a) was 3.9 eV (320 nm), which is close to the value registered for amorphous titanium oxide hydroxide (Cheng et al., 2014). Al_2O_3 having band-gap value (7.0 eV (Filatova et al., 2015)) cannot be detected in this range. After the addition of P25, the registered $dR/d\lambda$ curves and the evaluated band-gap values corresponded to P25. With the increase of the amount of immobilized P25 no significant optical changes were registered.

Heterogeneous photocatalytic measurements were carried out using ceramic sheets containing various amount of P25, such as P25-1, P25-2 and P25-3. There was no significant difference found on the transformation rate of monuron (max. 8 %), using P25-1, P25-2 and P25-3 samples. These results showed that, the 'active' surface of immobilized photocatlyst, which can be reached by the monuron, O_3 and UV light, could not be increased by this way. Due to these results, all further experiments were done using 0.777 $mg \cdot cm^{-2}$ catalyst surface loading when TiO_2 was applied in immobilized form. In this way, the amount of photocatalyst immobilized was the same as using TiO_2 in suspension, 1.0 $g \cdot dm^{-3}$ concentration, and 500 cm^3 total volume (Table 1, first row).

3.2. Reproducibility of the immobilization and the reusability of catalyst sheets

The reproducibility of the preparation of immobilized TiO_2 containing sheets was investigated by the photocatalytic transformation of monuron. Three P25-1, immobilized P25 containing ceramic sheets were made and tested by the same way. There was no significant difference among the measured transformation rates (less than 9%).

The reusability of this ceramic paper with immobilized TiO_2 in the case of simple photocatalysis was verified in the publication of Veréb et al. (2014). In our work the reusability of a TiO_2 containing sheet was tested by photocatalytic ozonation of monuron, using 10 $mg \cdot dm^{-3}$ gaseous O_3. The photocatalytic ozonation (imm-TiO_2/O_3, 10 $mg \cdot dm^{-3}$ O_3) was repeated three times, using the same P25-1 sheet. The transformation rate did not change significantly (max. 4%), confirming that the ceramic sheet can be reused even in the presence of O_3.

3.3. Transformation and mineralization rate of monuron

The comparison of the efficiency of ozonation, photocatalysis and photocatalytic ozonation using photocatalyst in both suspended and immobilized form was based on the initial transformation rates of monuron (Table 2).

The contribution of direct photolysis to the transformation of monuron was determined. The aqueous solution of monuron was irradiated for 60 min using the fluorescent light source. The results showed neither significant decrease in the concentration of monuron, nor change in the spectra of the treated samples. Consequently, the contribution of the direct photolysis to the transformation of monuron in UV irradiated suspension was negligible.

Reactivity of phenyl-urea pesticides toward O_3 decreases when Cl is attached to the aromatic ring due to the electro-attracting effect of chlorine, as presented by Benitez et al. (2007) and (Kovács et al., 2016a). In the case of the heterogeneous photocatalysis, the transformation of monuron was suggested to take place mainly through hydroxyl radicals (Krýsa et al., 2006) due to the negligible adsorption monuron and the high value of the rate constant of the reaction of monuron with hydroxyl radical ($7.3 \cdot 10^9$ $mol^{-1} \cdot dm^3 \cdot s^{-1}$ (Oturan et al., 2010)).

The immobilized form (imm-TiO_2/O_3) proved to be less effective compared to the suspended catalyst (susp-TiO_2/O_3) (Fig. 4 and Table 2). Suspended TiO_2 performs a high total surface area of TiO_2 per unit volume, while its immobilized form is often associated with mass transfer limitation over the TiO_2 layer. In our case the negative effect of immobilization is most likely because of the strongly decreased surface of P25 particles which can be reached by the monuron, O_3 and UV light.

In the present work the increasing amount of O_3 improved the transformation rate of monuron in each case (Table 2 and Fig. 4a-c.) and the initial rate of transformation depended linearly on the concentration of O_3 in gas phase (SUP4). Increasing the O_3 concentration improved the efficiency of the imm-TiO_2 process to a larger extent, as the addition of 20 $mg \cdot dm^{-3}$ O_3 increased the rate of transformation by up to ~6 times (from $8.1 \cdot 10^{-8}$ to $4.98 \cdot 10^{-7}$ $mol \cdot dm^{-3} \cdot s^{-1}$), whereas in the case of susp-TiO_2/O_3 this increase was only ~3 times (from $2.44 \cdot 10^{-7}$ to $6.86 \cdot 10^{-7}$ $mol \cdot dm^{-3} \cdot s^{-1}$). The increase of O_3 concentration from 5 $mg \cdot dm^{-3}$ to 20 $mg \cdot dm^{-3}$ itself also increased the reaction rate by up to ~5 times in the case of simple ozonation (from $7.8 \cdot 10^{-8}$ to $4.17 \cdot 10^{-7}$ $mol \cdot dm^{-3} \cdot s^{-1}$). In the case of TiO_2/O_3 method, the positive effect of added O_3 is most likely due to both the enhanced transformation rate of monuron via its direct reaction with molecular O_3. At the same time, using TiO_2/O_3 method, the relative contribution of the hydroxyl radicals formed via decomposition of dissolved O_3 on the surface of TiO_2 can be significant. Consequently, TiO_2 decreased the concentration of

dissolved O_3. This effect is more significant using TiO_2 in suspension because immobilization strongly decreases the surface of TiO_2. Moreover, the effect of O_3, as a more effective electron trap than O_2 must be also considered.

The relative contribution of hydroxyl radical based reactions to the monuron transformation can be determined by the effect of MeOH as hydroxyl radical scavenger on the initial transformation rate of monuron. The addition of MeOH decreased this value from 14.8 to 7.4 mol dm^{-3} s^{-1} using simple ozonation (c_{O3} = 10 mg·dm^{-3}). Consequently, the amount of monuron transformed via reaction with hydroxyl radical is commensurable with the amount of monuron transformed via reaction with O_3 even at pH 5.5. Similar conclusion was reported by Tahmasseb et al. (2001) under analogous conditions. We have also determined the MeOH effect at pH 11, when the decomposition of O_3 and the formation of hydroxyl radical are strongly enhanced by the hydroxide ions. In this case the effect of MeOH was more pronounced and decreased the initial rate from 28.3 to 8.3 mol·dm^{-3}·s^{-1}. Using heterogeneous photocatalysis (r_0 decreased from 24.4 to 5.07 mol·dm^{-3}·s^{-1}) or its combination with ozonation (r_0 decreased from 42.5 to 8.4 mol·dm^{-3}·s^{-1}), the considerable negative effect of MeOH confirmed that, the transformation is mainly due to the hydroxyl radical based reaction in both cases. These obtained values, together with the fact that the suspended TiO_2 decreased the dissolved O_3 concentration (Table 2), confirms that the addition of O_3 to the TiO_2 suspension enhances the rate of hydroxyl radical formation and the relative contribution of hydroxyl radical based reaction to the monuron degradation.

One of the main advantages of combining AOPs is the possible synergistic effect. We compared the initial transformation rates of monuron by using the combined processes with the sum of the transformation rates resulted by the corresponding separate methods. Although a minor increase (max. 10 %) in the efficiency of the combined methods could be seen, there was no significant synergism regarding to the transformation rate of monuron under the experimental conditions applied in this work. This could be due to the relative high contribution of the reaction with O_3 to the transformation of monuron. (Table 2) Similar conclusion was made by Farré et al. (2005) regarding the transformation rate of diuron. When monuron transformed completely, the decrease of the TOC reached 56% using suspended TiO_2 without O_3, while ozonation resulted in 31% mineralization at highest O_3 concentration (SUP5. and Fig. 4d-e). Byproducts formed mainly during heterogeneous photocatalysis via hydroxylation of aromatic ring (3-(4-chloro-hydroxyphenyl)-urea (Fig. 5a)) and *N*-demethylation (3-(4-chloro-hydroxyphenyl)-1-methyl urea) (Fig. 5b)). During ozonation the main intermediate was 3-(4-chlorophenyl)-1-methylurea (Fig. 5c), which

formed via *N*-demethylation. In case of the susp-TiO_2/O_3 method, O_3 strongly enhanced the rate of accumulation and decomposition of intermediates 3-(4-chloro-hydroxyphenyl)-1-methyl urea (Fig 5d) and 3-(hydroxy-4-chlorophenyl)-1,1-methyl urea (Fig. 5e). This observation is agreement with the enhanced TOC removal efficiency due to the increase of O_3 concentration. (Table 2. and Fig. 4). Tahmasseb (2002) suggested two main pathways of degradation during ozonation: *N*-demethylation and OH-substitution of a Cl atom on the phenyl ring. In addition, the transformation mechanism of monuron using heterogeneous photocatalysis includes the hydroxylation of the aromatic ring too (Bobu (2006), Fenoll (2013)). The intermediates identified in our work are in agreement with mechanisms suggested in these works. Considering the evolution of the concentration of detected by-products (Fig. 4 and 5.), their accumulation and decomposition seems to occur in parallel with the transformation of monuron.

Similar to the transformation rate of monuron, the efficiency of mineralization using combination of methods (susp-TiO_2/O_3) only slightly exceeded (with max. 14%) the sum of the mineralization efficiency of the susp-TiO_2 and ozonation. (SUP5.) The transformation and mineralization of the monuron can take place due to the reaction with molecular O_3, hydroxyl radicals and through the reaction of photogenerated charges with adsorbed monuron. The negative effect caused by the decreased concentration of dissolved O_3 due to the presence of TiO_2 (Table 2) was probably overcompensated by its positive effect on the concentration of formed hydroxyl radical due to the photocatalytic transformation of O_3.

3.4. Economic aspects of the applied processes

To compare the economic efficiency of the applied AOPs the values of E_{EO} were calculated for both monuron transformation (E_{EO}^{c}) (6a-c) and mineralization (E_{EO}^{TOC}) (6d-f).

The E_{EO} values decreased with the increase of O_3 concentration in each case (Fig. 6). The application of imm-TiO_2/O_3 resulted in significantly higher E_{EO}^{c} values than ozonation or susp-TiO_2/O_3 process (Fig 6c), mainly at lower concentrations of O_3. There was no significant difference between the energy requirement of ozonation and susp-TiO_2/O_3 process regardless of the O_3 concentration. However, it should be noted, that the energy requirement of TiO_2 separation from suspension was not taken into account. The energy requirement of microfiltration of P25 is about 100 - 300 $kWh \cdot m^{-3}$ and depends strongly on the operation conditions (type of membrane, transmembrane pressure, filtration rate, etc). This value can be decreased with the combination of filtration with vibration (Massé et al., 2011) or coagulation (Judd et al., 2001). In our study, the E_{EO}^{c} value determined for both susp-TiO_2 (30 $kWh \cdot m^{-}$

^{3}·order^{-1}) and imm-TiO_2 processes (85 kWh·m^{-3}·order^{-1}) are lower than the estimated energy requirement of microfiltration. Moreover, the difference between thes E_{EO}^{c} values of susp-TiO/O_3 and imm-TiO/O_3 is definitely lower than the minimum energy requirement of microfiltration (100 kWh·m^{-3}) of TiO_2. Consequently, the running cost of imm-TiO_2/O_3 method must be lower than the sum of the running cost of microfiltration and susp-TiO_2/O_3 method.

The combination of susp-TiO_2 with ozonation only slightly enhanced the efficiency of both transformation and mineralization rates (Table 2 and Fig. 4), and its economic efficiency corresponded to ozonation, as proved by E_{EO}^{c} values (Fi. 6c). However, the significant positive effect of the O_3 addition to the irradiated susp-TiO_2 is well manifested in E_{EO}^{TOC} values (Fig. 6f) even at high O_3 concentrations. Using either 15 or 20 mg·dm^{-3} O_3, the E_{EO}^{c} and E_{EO}^{TOC} values are comparable (Fig. c and f). As Fig. 4 shows the decrease of monuron concentration takes place parallel with decrease of the TOC content, with similar rate in these cases. There was no significant difference between E_{EO}^{c} values for ozonation and the susp-TiO_2/O_3 process (Fig.), opposed to the E_{EO}^{TOC} values (Fig. 6f), where the combined process proved to be superior and required only the 30-34% of the E_{EO}^{TOC} value of the ozonation using either 15 or 20 mg·dm^{-3} O_3.

When immobilized catalyst is used, the E_{EO}^{TOC} values were the highest. Comparing the E_{EO}^{TOC} values, the following observations can be made: addition of O_3 at highest concentration (20 mg·dm^{-3}) decreased ~50% the E_{EO}^{TOC} value compared to imm-TiO_2 (from 573 to 306 kWh·dm^{-3}·order^{-1}). However, the E_{EO}^{TOC} of imm-TiO_2/O_3 (306 kWh·dm^{-3}·order^{-1}) was more than two times higher than the E_{EO}^{TOC} of simple ozonation (130 kWh·dm^{-3}·order^{-1}), and about seven times higher than the energy requirement of susp-TiO_2/O_3 (44 kWh·dm^{-3}·order^{-1}) (Fig. f). Moreover, the value of E_{EO}^{TOC} of imm-TiO_2/O_3 (285 - 306 kWh·m^{-3}·order^{-1}) is commensurable or most probably higher than the sum of the minimum energy requirement of filtration and E_{EO}^{TOC} related to the application of susp-TiO_2/O_3 (213 - 144 kWh·m^{-3}·order^{-1}).

4. Conclusions

In this study the transformation and mineralization of monuron and the economic feasibility of various AOPs, such as heterogeneous photocatalysis, using photocatalyst in suspensions and in immobilized form, ozonation, and their combination at various O_3 concentrations (0–

20 mg·dm^{-3}) were investigated. Ceramic sheets containing well fixed P25 were characterized by XRD, DRS and SEM measurements.

However significant synergism was not observed, kinetic measurements proved that addition of O_3 increased the rate of both transformation and mineralization. To compare the methods from economic aspect, E_{EO} values related to the decrease of monuron concentration (E_{EO}^{c}) and TOC content (E_{EO}^{TOC}) were calculated. Both E_{EO}^{c} and E_{EO}^{TOC} values decreased with the increase of O_3 concentration. There was no significant difference between E_{EO}^{c} values for ozonation and the susp-TiO_2/O_3 process, opposed to the E_{EO}^{TOC} values, where the combined process proved to be superior and required only ~30% of the E_{EO}^{TOC} value of the ozonation.

5. Acknowledgement

G. Veréb acknowledges the support of the János Bolyai Research Scholarship of the Hungarian Academy of Sciences. The support of the Swiss Contribution (SH7/2/20) and Bilateral Scientific and Technology (S&T) cooperation between Hungary and India (TÉT_15_IN-1-2016-0013) is acknowledged and greatly appreciated.

6. References

Aguinaco, A., Beltrán, F.J., García-Araya, J.F., Oropesa, A., 2012. Photocatalytic ozonation to remove the pharmaceutical diclofenac from water: Influence of variables. Chem. Eng. J. 189-190, 275-282. 10.1016/j.cej.2012.02.072

Bader, H., Hoigné, J., 1981. Determination of ozone in water by the indigo method. Water Res. 15, 449-456. 10.1016/0043-1354(81)90054-3

Baia, L., Vulpoi, A., Radu, T., Karácsonyi, É., Dombi, A., Hernádi, K., Danciu, V., Simon, S., Norén, K., Canton, S.E., Kovács, G., Pap, Z., 2014. TiO_2/WO_3/Au nanoarchitectures' photocatalytic activity "from degradation intermediates to catalysts' structural peculiarities" Part II: Aerogel based composites – fine details by spectroscopic means. Appl. Catal., B. 148-149, 589-600. 10.1016/j.apcatb.2013.12.034

Balasubramanian, G., Dionysiou, D., Suidan, M., Baudin, I., Laine, J., 2004. Evaluating the activities of immobilized TiO_2 powder films for the photocatalytic degradation of organic contaminants in water. Appl. Catal., B 47, 73-84. 10.1016/j.apcatb.2003.04.002

Baudys, M., Krýsa, J., Mills, A., 2017. Smart inks as photocatalytic activity indicators of self-cleaning paints. Catal. Today 280, 8-13. 10.1016/j.cattod.2016.04.041

Behnajady, M.A., Modirshahla, N., Mirzamohammady, M., Vahid, B., Behnajady, B., 2008. Increasing photoactivity of titanium dioxide immobilized on glass plate with optimization of heat attachment method parameters. J. Hazard. Mater. 160, 508-513. 10.1016/j.jhazmat.2008.03.049

Beltrán, F.J., Rivas, F.J., Gimeno, O., 2005. Comparison between photocatalytic ozonation and other oxidation processes for the removal of phenols from water. J. Chem. Technol. Biotechnol. 80, 973-984. 10.1002/jctb.1272

Benitez, F.J., Garcia, C., Acero, J.L., Real, F.J., 2009. Removal of phenylurea herbicides from waters by using chemical oxidation treatments. World Acad. Sci. Eng. Technol. 3, 648-656

Benitez, F.J., Real, F.J., Acero, J.L., Garcia, C., 2007. Kinetics of the transformation of phenyl-urea herbicides during ozonation of natural waters: rate constants and model predictions. Water Res. 41, 4073-4084. 10.1016/j.watres.2007.05.041

Bobu, M., Wilson, S., Greibrokk, T., Lundanes, E., Siminiceanu, I., 2006. Comparison of advanced oxidation processes and identification of monuron photodegradation

products in aqueous solution. Chemosphere 63, 1718-1727. 10.1016/j.chemosphere.2005.09.034

Bolton, J.R., Bircher, K.G., Tumas, W., Tolman, C.A., 2001. Figures-of-merit for the technical development and application of advanced oxidation technologies for both electric- and solar-driven systems (IUPAC Technical Report). Pure Appl. Chem. 73. 10.1351/pac200173040627

Bonnemoy, F., Lavédrine, B., Boulkamh, A., 2004. Influence of UV irradiation on the toxicity of phenylurea herbicides using Microtox® test. Chemosphere 54, 1183-1187. 10.1016/j.chemosphere.2003.10.027

Cardoso, J.C., Bessegato, G.G., Boldrin Zanoni, M.V., 2016. Efficiency comparison of ozonation, photolysis, photocatalysis and photoelectrocatalysis methods in real textile wastewater decolorization. Water Res. 98, 39-46. 10.1016/j.watres.2016.04.004

Černigoj, U., Štangar, U.L., Trebše, P., 2007. Degradation of neonicotinoid insecticides by different advanced oxidation processes and studying the effect of ozone on TiO_2 photocatalysis. Appl. Catal., B 75, 229-238. 10.1016/j.apcatb.2007.04.014

Cheng, C., Amini, A., Zhu, C., Xu, Z., Song, H., Wang, N., 2014. Enhanced photocatalytic performance of TiO_2-ZnO hybrid nanostructures. Sci. Rep. 4, 4181. 10.1038/srep04181

Chiou, C.F., Mariñas, B.J., Adams, J.Q., 1995. Modified indigo method for gaseous and aqueous ozone analyses. Ozone Sci. Eng. 17, 329-344. 10.1080/01919519508547539

Chu, W., Rao, Y.F., 2012. Photocatalytic oxidation of monuron in the suspension of WO_3 under the irradiation of UV-visible light. Chemosphere 86, 1079-1086. 10.1016/j.chemosphere.2011.11.062

Dunlop, P.S.M., McMurray, T.A., Hamilton, J.W.J., Byrne, J.A., 2008. Photocatalytic inactivation of Clostridium perfringens spores on TiO_2 electrodes. J. Photochem. Photobiol., A 196, 113-119. 10.1016/j.jphotochem.2007.11.024

Fabiyi, M.E., Skelton, R.L., 2000. Photocatalytic mineralisation of methylene blue using buoyant TiO_2-coated polystyrene beads. J. Photochem. Photobiol., A 132, 121-128. 10.1016/s1010-6030(99)00250-6

Farré, M.J., Franch, M.I., Malato, S., Ayllon, J.A., Peral, J., Domenech, X., 2005. Degradation of some biorecalcitrant pesticides by homogeneous and heterogeneous photocatalytic ozonation. Chemosphere 58, 1127-1133. 10.1016/j.chemosphere.2004.09.064

Fathinia, M., Khataee, A.R., Aber, S., Naseri, A., 2016. Development of kinetic models for photocatalytic ozonation of phenazopyridine on TiO_2 nanoparticles thin film in a mixed semi-batch photoreactor. Appl. Catal., B 184, 270-284. 10.1016/j.apcatb.2015.11.033

Fenoll, J., Sabater, P., Navarro, G., Pérez-Lucas, G., Navarro, S., 2013. Photocatalytic transformation of sixteen substituted phenylurea herbicides in aqueous semiconductor suspensions: Intermediates and degradation pathways. J. Haz. Mat. 244– 245, 370–379 10.1016/j.jhazmat.2012.11.055

Filatova, E.O., Konashuk, A.S., 2015. Interpretation of the changing the band gap of Al_2O_3 depending on Its crystalline form: connection with different local symmetries. J. Phys. Chem., C. 119(35) , 20755-20761. 10.1021/acs.jpcc.5b06843

Flak, D., Braun, A., Mun, B.S., Park, J.B., Parlinska-Wojtan, M., Graule, T., Rekas, M., 2013. Spectroscopic assessment of the role of hydrogen in surface defects, in the electronic structure and transport properties of TiO_2, ZnO and SnO_2 nanoparticles. Phys. Chem. Chem. Phys. 15, 1417-1430. 10.1039/c2cp42601c

Gelover, S., Mondragón, P., Jiménez, A., 2004. Titanium dioxide sol–gel deposited over glass and its application as a photocatalyst for water decontamination. J. Photochem. Photobiol., A 165, 241-246. 10.1016/j.jphotochem.2004.03.023

Giornelli, T., Löfberg, A., Guillou, L., Paul, S., Lecourtois, V., Bordesrichard, E., 2007. Catalytic wall reactor: Catalytic coatings of stainless steel by VO_x/TiO_2 and Co/SiO_2 catalysts. Catal. Today 128, 201-207. 10.1016/j.cattod.2007.07.023

Hart, E.J., Sehested, K., Holoman, J., 1983. Molar absorptivities of ultraviolet and visible bands of ozone in aqueous solutions. Anal. Chem. 55, 46-49. 10.1021/ac00252a015

Hatchard, C.G., Parker, C.A., 1956. A new sensitive chemical actinometer II.: Potassium ferrioxalate as a standard chemical actinometer. Proc. Royal Soc. 235, 518-536. 10.1098/rspa.1956.0102

Hegedűs, P., Szabó-Bárdos, E., Horváth, O., Horváth, K., Hajós, P., 2015. TiO_2-mediated photocatalytic mineralization of a non-ionic detergent: comparison and combination with other advanced oxidation procedures. Materials 8, 231-250. 10.3390/ma8010231

Hosseini, S.N., Borghei, S.M., Vossoughi, M., Taghavinia, N., 2007. Immobilization of TiO_2 on perlite granules for photocatalytic degradation of phenol. Appl. Catal., B 74, 53-62. 10.1016/j.apcatb.2006.12.015

Ilisz, I., Bokros, A., Dombi, A., 2004. TiO_2-based heterogeneous photocatalytic water treatment combined with ozonation. Ozone Sci. Eng. 26, 585-594. 10.1080/01919510490885406

Jing, Y., Li, L., Zhang, Q., Lu, P., Liu, P., Lu, X., 2011. Photocatalytic ozonation of dimethyl phthalate with TiO_2 prepared by a hydrothermal method. J. Hazard. Mater. 189, 40-47. 10.1016/j.jhazmat.2011.01.132

Judd, S.J., Hillis, P., 2001. Optimisation of combined coagulation and microfiltration for water treatment. Water Res. 35, 2895-2904. 10.1016/s0043-1354(00)00586-8

Karches, M., Morstein, M., Rudolf von Rohr, P., Pozzo, R.L., Giombi, J.L., Baltanás, M.A., 2002. Plasma-CVD-coated glass beads as photocatalyst for water decontamination. Catal. Today 72, 267-279. 10.1016/s0920-5861(01)00505-3

Khataee, A.R., Fathinia, M., Joo, S.W., 2013. Simultaneous monitoring of photocatalysis of three pharmaceuticals by immobilized TiO_2 nanoparticles: chemometric assessment, intermediates identification and ecotoxicological evaluation. Spectrochim. Acta, A 112, 33-45. 10.1016/j.saa.2013.04.028

Klare, M., Waldner, G., Bauer, R., Jacobs, H., Broekaert, J.A.C., 1999. Degradation of nitrogen containing organic compounds by combined photocatalysis and ozonation. Chemosphere 38, 2013-2027. 10.1016/s0045-6535(98)00414-7

Kopf, P., Gilbert, E., Eberle, S.H., 2000. TiO_2 photocatalytic oxidation of monochloroacetic acid and pyridine: influence of ozone. J. Photochem. Photobiol., A 136, 163-168. 10.1016/s1010-6030(00)00331-2

Kottuparambil, S., Lee, S.Y., Han, T., 2013. Single and interactive effects of the antifouling booster herbicides diuron and Irgarol 1051 on photosynthesis in the marine cyanobacterium, Arthrospira maxima. Toxicol. Environ. Health Sci. 5, 71-81. 10.1007/s13530-013-0157-6

Kovács, G., Baia, L., Vulpoi, A., Radu, T., Karácsonyi, É., Dombi, A., Hernádi, K., Danciu, V., Simon, S., Pap, Z., 2014a. TiO_2/WO_3/Au nanoarchitectures' photocatalytic activity, "from degradation intermediates to catalysts' structural peculiarities", Part I: Aeroxide P25 based composites. Appl. Catal., B 147, 508-517. 10.1016/j.apcatb.2013.09.019

Kovács, K., Farkas, J., Veréb, G., Arany, E., Simon, G., Schrantz, K., Dombi, A., Hernádi, K., Alapi, T., 2016a. Comparison of various advanced oxidation processes for the degradation of phenylurea herbicides. J. Environ. Sci. Health, B., 1-10. 10.1080/03601234.2015.1120597

Kovács, K., He, S., Míle, V., Földes, T., Pápai, I., Takács, E., Wojnárovits, L., 2016b. Ionizing radiation induced degradation of monuron in dilute aqueous solution. Rad. Phys. Chem. 124, 191-197. 10.1016/j.radphyschem.2015.10.028

Kovács, K., Míle, V., Csay, T., Takács, E., Wojnárovits, L., 2014b. Hydroxyl radical-induced degradation of fenuron in pulse and gamma radiolysis: kinetics and product analysis. Environ. Sci. Pollut. Res. Int. 21, 12693-12700. 10.1007/s11356-014-3197-9

Krýsa, J., Waldner, G., Měšťánková, H., Jirkovský, J., Grabner, G., 2006. Photocatalytic degradation of model organic pollutants on an immobilized particulate TiO_2 layer. Appl. Catal., B 64, 290-301. 10.1016/j.apcatb.2005.11.007

Massé, A., Thi, H.N., Legentilhomme, P., Jaouen, P., 2011. Dead-end and tangential ultrafiltration of natural salted water: Influence of operating parameters on specific energy consumption. J. Mem. Sci. 380, 192-198. 10.1016/j.memsci.2011.07.002

Mehrjouei, M., Müller, S., Möller, D., 2014a. Catalytic and photocatalytic ozonation of tert-butyl alcohol in water by means of falling film reactor: Kinetic and cost–effectiveness study. Chem. Eng. J. 248, 184-190. 10.1016/j.cej.2014.03.047

Mehrjouei, M., Müller, S., Möller, D., 2014b. Energy consumption of three different advanced oxidation methods for water treatment: a cost-effectiveness study. J. Cleaner Prod. 65, 178-183. 10.1016/j.jclepro.2013.07.036

Mehrjouei, M., Müller, S., Möller, D., 2015. A review on photocatalytic ozonation used for the treatment of water and wastewater. Chem. Eng. J. 263, 209-219. 10.1016/j.cej.2014.10.112

Melián, E.P., Díaz, O.G., Rodríguez, J.M., Araña, J., Peña, J.P., 2013. Adsorption and photocatalytic degradation of 2,4-dichlorophenol in TiO_2 suspensions. Effect of hydrogen peroxide, sodium peroxodisulphate and ozone. Appl. Catal., A 455, 227-233. 10.1016/j.apcata.2013.02.007

Mestankova, H., Escher, B., Schirmer, K., von Gunten, U., Canonica, S., 2011. Evolution of algal toxicity during (photo)oxidative degradation of diuron. Aquat. Toxicol. 101, 466-473. 10.1016/j.aquatox.2010.10.012

Naskar, S., Pillay, S.A., Chanda, M., 1998. Photocatalytic degradation of organic dyes in aqueous solution with TiO_2 nanoparticles immobilized on foamed polyethylene sheet. J. Photochem. Photobiol., A 113, 257-264. 10.1016/s1010-6030(97)00258-x

Ohtani, B., Prieto-Mahaney, O.O., Li, D., Abe, R., 2010. What is Degussa (Evonik) P25? Crystalline composition analysis, reconstruction from isolated pure particles and

photocatalytic activity test. J. Photochem. Photobiol., A 216, 179-182. 10.1016/j.jphotochem.2010.07.024

Oturan, M.A., Edelahi, M.C., Oturan, N., El kacemi, K., Aaron, J., 2010. Kinetics of oxidative degradation/mineralization pathways of the phenylurea herbicides diuron, monuron and fenuron in water during application of the electro-Fenton process. Appl. Catal., B 97, 82-89. 10.1016/j.apcatb.2010.03.026

Pap, Zs., Mogyorósi, K., Veréb, G., Dombi, A., Hernádi, K., Danciu, V., Baia, L., 2014. Commercial and home-made nitrogen modified titanias. A short reflection about the advantageous/disadvantageous properties of nitrogen doping in the frame of their applicability. J. Mol. Structure 1073, 157-163. 10.1016/j.molstruc.2014.05.023Pichat, P., Cermenati, L., Albini, A., Mas, D., Delprat, H., Guillard, C., 2000. Degradation processes of organic compounds over UV-irradiated TiO_2. Effect of ozone. Res. Chem. Intermediat. 26, 161-170. 10.1163/156856700x00200

Puma, G.L., Bono, A., Krishnaiah, D., Collin, J.G., 2008. Preparation of titanium dioxide photocatalyst loaded onto activated carbon support using chemical vapor deposition: a review paper. J. Hazard. Mater. 157, 209-219. 10.1016/j.jhazmat.2008.01.040

Rao, Y.F., Chu, W., 2010. Degradation of linuron by UV, ozonation, and UV/O_3 processes - effect of anions and reaction mechanism. J. Hazard. Mater. 180, 514-523. 10.1016/j.jhazmat.2010.04.063

Sánchez, L., Peral, J., Domènech, X., 1998. Aniline degradation by combined photocatalysis and ozonation. Appl. Catal., B 19, 59-65. 10.1016/s0926-3373(98)00058-7

Solís, R.R., Rivas, F.J., Martínez-Piernas, A., Agüera, A., 2016. Ozonation, photocatalysis and photocatalytic ozonation of diuron. Intermediates identification. Chem. Eng. J. 292, 72-81. 10.1016/j.cej.2016.02.005

Tahmasseb, A.L., Nélieu, S., Kerhoas, L., Einhorn, J., 2002. Ozonation of chlorophenylurea pesticides in water: reaction monitoring and degradation pathways. Sci. Total Environ. 291, 33-44. 10.1016/s0048-9697(01)01090-7

Tryba, B., 2008. Immobilization of TiO_2 and Fe-C-TiO_2 photocatalysts on the cotton material for application in a flow photocatalytic reactor for decomposition of phenol in water. J. Hazard. Mater. 151, 623-627. 10.1016/j.jhazmat.2007.06.034

Veréb, G., Ambrus, Z., Pap, Z., Mogyorósi, K., Dombi, A., Hernádi, K., 2014. Immobilization of crystallized photocatalysts on ceramic paper by titanium(IV) ethoxide and photocatalytic decomposition of phenol. React. Kinet., Mech. Catal. 113, 293-303. 10.1007/s11144-014-0734-y

Xiao, J., Xie, Y., Cao, H., 2015. Organic pollutants removal in wastewater by heterogeneous photocatalytic ozonation. Chemosphere 121, 1-17. 10.1016/j.chemosphere.2014.10.072

Zhang, T., Luo, Y., Jia, B., Li, Y., Yuan, L., Yu, J., 2015. Immobilization of self-assembled pre-dispersed nano-TiO_2 onto montmorillonite and its photocatalytic activity. J. Environ. Sci. 32, 108-117. 10.1016/j.jes.2015.01.010

Zhang, X., Lei, L., 2008. Effect of preparation methods on the structure and catalytic performance of TiO_2/AC photocatalysts. J. Hazard. Mater. 153, 827-833. 10.1016/j.jhazmat.2007.09.052

Figure captions

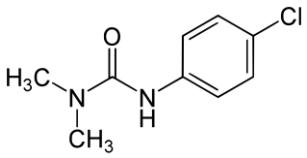

Fig. 1 The chemical structure of monuron (*3*-(*p*-chlorophenyl)-*1,1*-dimethylurea)

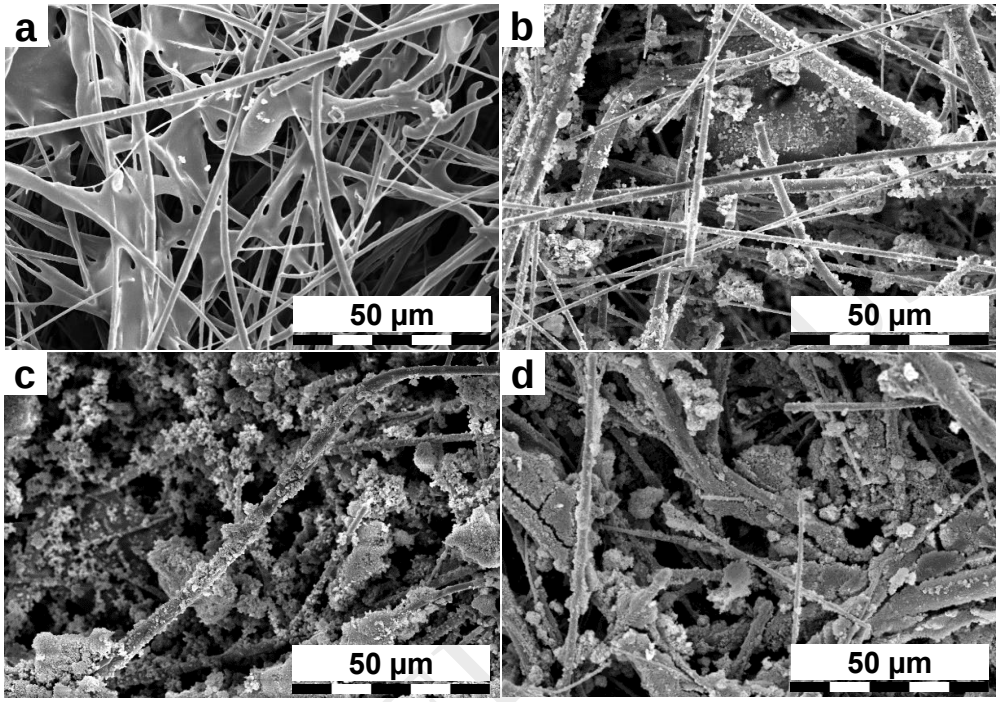

Fig. 2 SEM images of the bare ceramic paper (a) and the ceramic papers containing various amount of immobilized TiO_2 (P25-1 (0.777 mg·cm^{-2}) (b); P25-2 (1.555 mg·cm^{-2}) (c); and P25-3 (2.332 mg·cm^{-2}) (d)

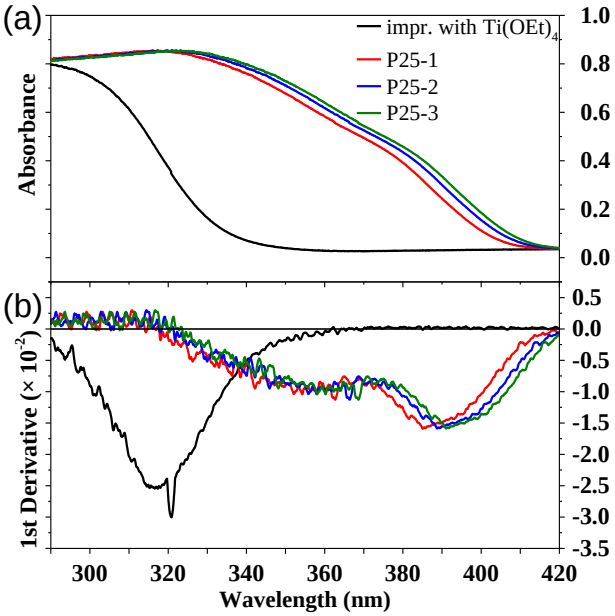

Fig. 3 The DRS spectra (a) and their derivative curves (b) of the ceramic paper impregnated with $Ti(OEt)_4$ and the ceramic papers containing various amount of immobilized P25 (P25-1: 0.755 mg·cm^{-2}; P25-2: 1.445 mg·cm^{-2}; P25-3: 2.315 mg·cm^{-2} (measured values))

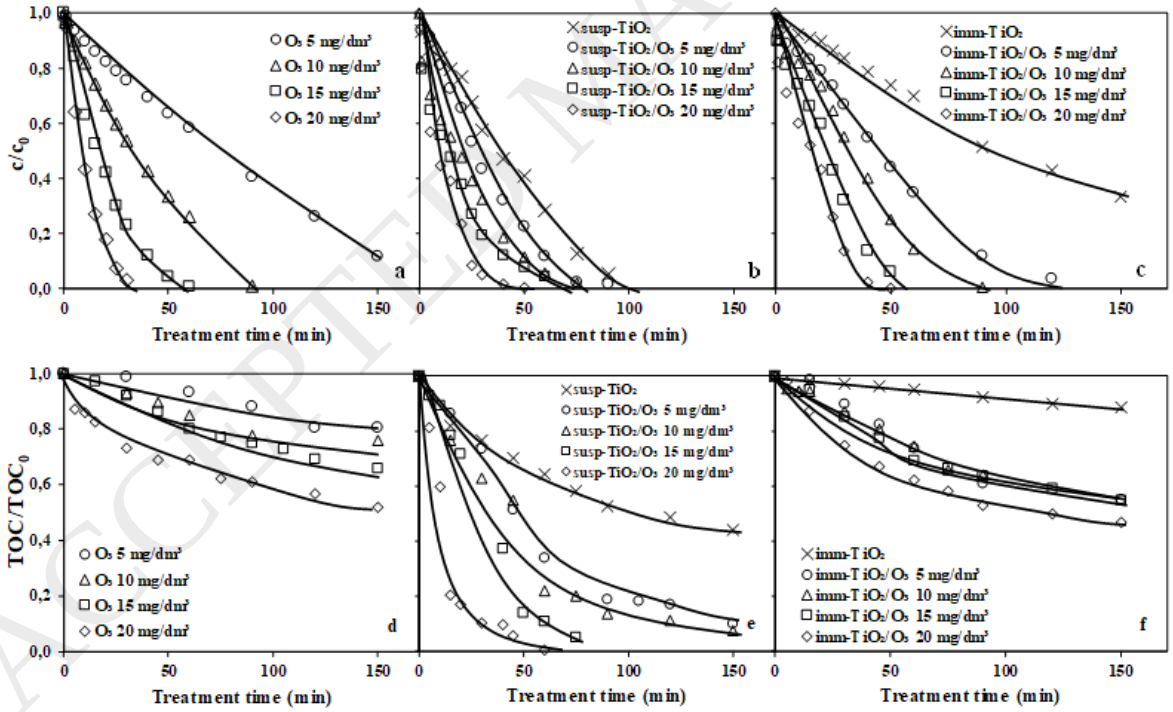

Fig. 4 The relative concentration (c/c_0) of monuron (a, b and c) and the relative TOC content (TOC/TOC_0) of the treated solutions (d, e and f) versus the time of treatment

a, d: ozonation; b, e: susp-TiO_2/O_3; c, f: imm-TiO_2/O_3

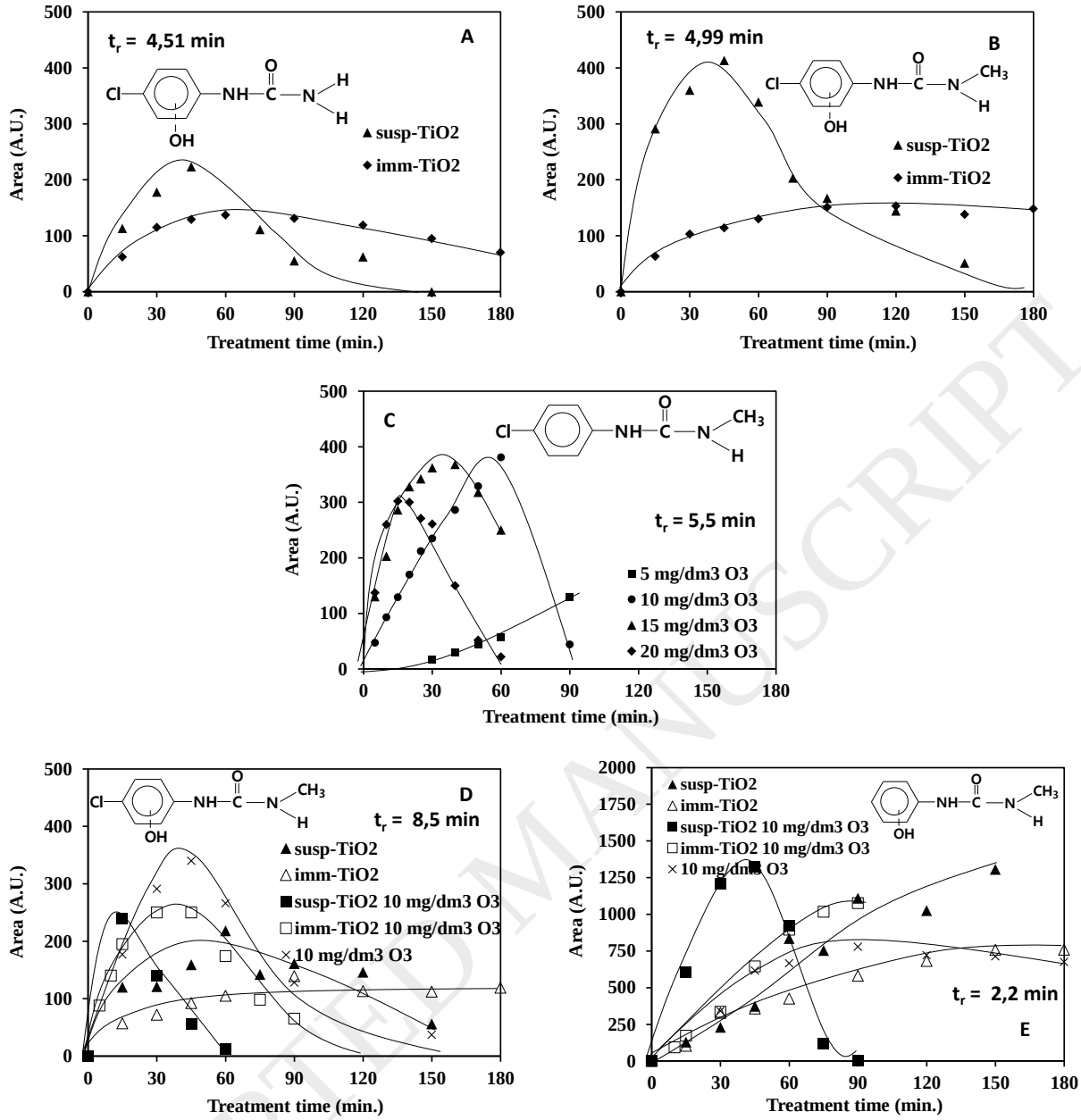

Fig 5 The of chromatographic peaks of formed intermediates (A: 3-(4-chloro-hydroxyphenyl)-urea; B: 3-(4-chloro-hydroxyphenyl)-1-methyl urea C: 3-(4-chlorophenyl)-1-methylurea; D: 3-(4-chloro-hydroxyphenyl)-1-methyl urea (stereoisomer of B) E: 3-(hydroxy-4-chlorophenyl)-1,1-methyl urea) versus time of treatment

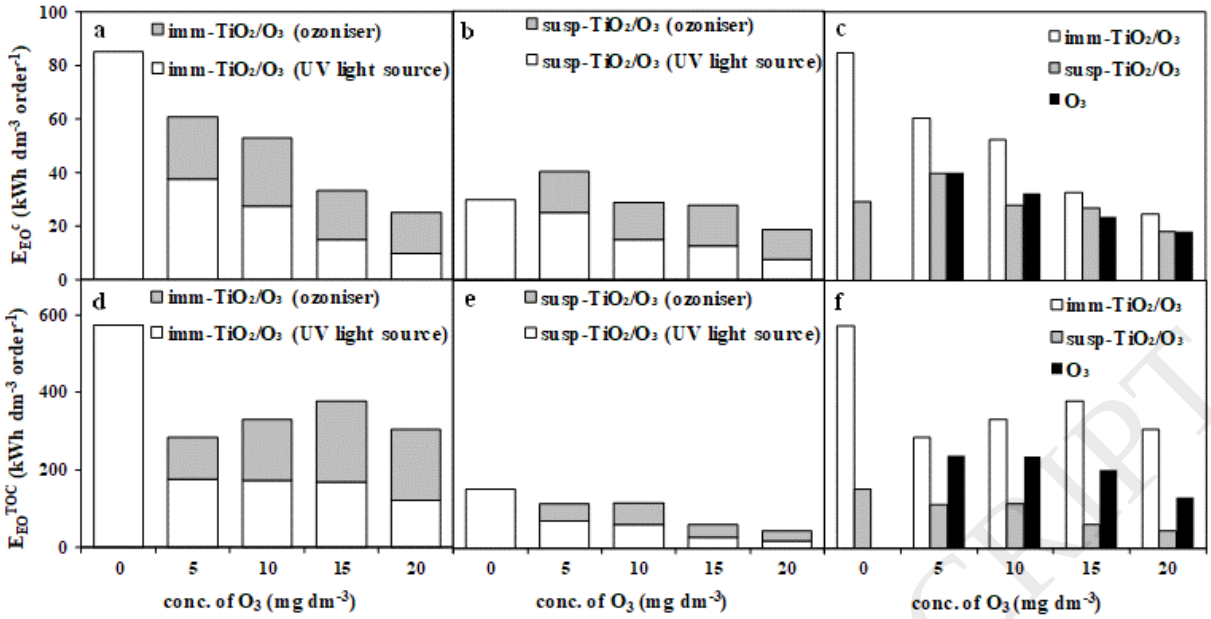

Fig. 6 The E_{EO}^{c} values determined for monuron transformation and E_{EO}^{TOC} values determined for monuron mineralization: E_{EO}^{c}, imm-TiO_2/O_3 (a), E_{EO}^{c}, susp-TiO_2/O_3 (b) (white: the part of E_{EO}^{c} required by the UV light source; grey: the part of E_{EO} required by the ozonizer) and the values of E_{EO}^{c} of each methods (c), E_{EO}^{TOC}, imm-TiO_2/O_3 (d), E_{EO}^{TOC}, susp-TiO_2/O_3 (e) and the values of E_{EO}^{TOC} to compare the methods (f)

Table 1 Calculated and measured amount of TiO_2 immobilized on ceramic sheets

Sample name	TiO_2 immobilized (calculated) ($mg \cdot cm^{-2}$) / (mg)	TiO_2 immobilized (measured) ($mg \cdot cm^{-2}$) / (mg)
P25-1	0.777 / 370	0.755 / 359
P25-2	1.555 / 740	1.445 / 688
P25-3	2.332 / 1110	2.315 / 1102

Table 2 The initial transformation rates of monuron (r_0) and the corresponding equilibrium concentrations of dissolved O_3 (c_{O_3})

	Initial rates of transformation (r_0 ($\times 10^{-8}$ $mol \cdot dm^{-3} \cdot s^{-1}$)) and equilibrium concentrations of dissolved O_3 (c_{o_3} ($mg \cdot dm^{-3}$))					
c_{O_3} in gas phase ($mg \cdot dm^{-3}$)		**0**	**5**	**10**	**15**	**20**
ozonation	**r_0**	–	**7.8±0.4**	**14.8±0.5**	**24.4±1.6**	**41.7±4.5**
	c_{o_3}	–	2.0±0.1	3.8±0.1	5.1±0.1	10.3±0.0
photocatalytic ozonation using TiO_2 in suspension (susp-TiO_2/O_3.)	**r_0**	**24.4±2.2**	31.7±2.6	42.5±4.2	49.6±4.7	68.1±6.8
	c_{o_3}	–	1.3±0.0	2.0±0.1	3.1±0.1	7.8±0.3
photocatalytic ozonation using TiO_2 in immobilized form (imm-TiO_2/O_3.)	**r_0**	**8.1±1.0**	16.1±1.5	24.8±4.1	34.6±1.5	49.8±4.1
	c_{o_3}	–	1.2±0.0	2.2±0.1	4.1±0.3	8.9±0.2